**Supplementary Materials and Methods**

***Antibodies and Reagents:*** anti-p300 (N-15) (sc-584; Santa Cruz Biotechnology, Dallas, TX), anti-fibronectin (610077; BD Biosciences, San Jose, VA), anti-SMAD2/3 (sc-133098; Santa Cruz Biotechnology), anti-SMAD2/3 (3102; Cell Signaling Technology, Danvers, MA), anti-SMAD2 (86F7) (3122; Cell Signaling Technology), anti-SMAD3 (c67H9) (9523; Cell Signaling Technology), anti-α-SMA (A5228; MilliporeSigma, Burlington, MA), anti-α-SMA (ab5694, Abcam, Cambridge, UK), anti-PDGFR-α (3170; Cell Signaling Technology), anti-HDAC2 (C-19) (sc-6296; Santa Cruz Biotechnology), anti-TβRII (K105) (3713; Cell Signaling Technology), anti-DYKDDDDK (FLAG tag) (2368; Cell Signaling Technology), anti-P-SMAD2 (3101; Cell Signaling Technology), anti-TAZ (560235; BD Biosciences), anti-YAP1 (4912; Cell Signaling Technology), anti-β-actin (A5441; MilliporeSigma), and anti-GAPDH (G8140; US Biological, Salem, MA), anti-tenascin C (sc-20932; Santa Cruz Biotechnology), anti-periostin (sc-67233; Santa Cruz Biotechnology), anti-CTGF (sc-14939; Santa Cruz Biotechnology), anti-E-cadherin (61081; BD Biosciences), anti-FLAG (M2) (F1804; MilliporeSigma), anti-FLAG (M2)-FITC (F4049; MilliporeSigma), anti-fibronectin (ab2413; Abcam), anti-HSC70 (sc-7298; Santa Cruz Biotechnology), anti-FGF-2(C-2) (sc-74412; Santa Cruz Biotechnology), anti-TAZ(D-8)-AF594 (sc-518026; Santa Cruz Biotechnology), and anti-SMAD2/3(C-8)-AF594 (sc-133098; Santa Cruz Biotechnology).

TGFβ1 was from R & D (240-B; R & D Systems, Inc. Minneapolis, MN). C646 was purchased from AdipoGen (AG-CR1-3508; AdipoGen Corporation, San Diego, CA).

FLAG-tagged TGFβ receptor I (TβRI-FLAG) cDNA was inserted into the pMMP retroviral vector by standard subcloning procedures and confirmed by sequencing (1, 2). FLAG-tagged p300 wildtype cDNA was a gift from Dr. Makiko Fujii (3). P300 NLS-deletion mutant with amino acids

11-PSAKRPK-17 removed was generated using a Q5 Site-Directed Mutagenesis kit. Deletion of the NLS was confirmed by sequencing.

***SiRNA and shRNA:*** YAP1 siRNA (SI00084567 and SI02662954), TAZ siRNA (SI00111216 and SI001112300) and control siRNA (SI03650318) were from Qiagen (Hilden Germany). P300 shRNA lentiviral constructs were from MISSION shRNA Library (NM_001429.1-7724s1c1, NM_001429.1-3602s1c1, and NM_001429.1-2773s1c1; MilliporeSigma). A construct encoding non-target shRNA (SHC202; MilliporeSigma) was used to package control lentiviruses.

***Transfection of plasmid or siRNA and viral transduction of cells.*** Both FLAG-p300wt and FLAG-p300NLS-Del were transfected into LX2 cells by Effectene Transfection Reagent (301425; Qiagen), according to a manufacture-recommended protocol. Cells were collected 48-72 hours later for analyses. SiRNAs were transfected into HSCs by Oligofectamine Reagent (12252011; Thermo Fisher Scientific, Waltham, MA), and cells were collected at 72-96 hours later for experiments. Retroviruses or lentiviruses were generated by cotransfecting 293T cells with 2-3 plasmids by Effectene Transfection Reagent, as we have described (1, 2, 4, 5). Viral transduction of HSCs was done by incubating cells with viral supernatant (25% - 50%) containing polybrene (8 μg/ml) overnight and cells were collected for experiments 72 hours later.

***Immunofluorescence (IF) and microscopy:*** Cultured cells were fixed by 4% paraformaldehyde for 10 minutes followed by permeabilization by 0.2% Triton X-100 for 3 minutes before staining. For staining of murine tumor biopsies, tumors were first sectioned at 7 μm using a Leica cryostat. After sections were dried at room temperature overnight, they were fixed by 4% paraformaldehyde

for 10 minutes. Subsequently, cells or sections were incubated with a primary antibody at 4°C overnight and a secondary antibody conjugated with Alexa Fluor (Thermo Fisher Scientific) was added for detection (1, 4). Cell nuclei were counterstained with DAPI dye. Fluorescence microscopy was performed with a Nikon Eclipse TE2000-E microscope (Nikon, Tokyo, Japan) or Axio observer (Zeiss, Oberkochen, Germany) (6). IF signals were quantitated using the ImageJ software (NIH).

***Western blot analysis (WB), nuclear fractionation, and coimmunoprecipitation (coIP):*** Cultured cells or murine tumor tissues were lysed with RIPA buffer, containing PMSF, $Na_2VO_3$, NaF, and protease inhibitors (11873580001; Roche, Penzberg, Germany) for WB. After homogenization and incubation for 20 minutes on ice, lysates were collected and cleared by centrifugation. Protein concentrations were quantitated by a DC™ Protein Assay kit (5000111; Bio-Rad, Hercules, CA) and 5-15 μg of total protein was loaded into each well of a PAGE gel for electrophoresis. Blotting and antibody incubation were performed as we previously described (2, 5) and signals were captured by an Amersham imager 600 (GE Healthcare Life Sciences). Densitometry analysis was performed with the ImageJ software (NIH, Bethesda, MA).

Cell nuclei were isolated using CelLytic NuCLEAR Extraction Kit (NXTRACT; MilliporeSigma). In brief, cell pellets were resuspended in Hypotonic Lysis Buffer and IGEPAL CA-630 detergent was added in to lyse the cells. After centrifugation at 10,000 *g*, supernatant containing cytoplasmic proteins was collected. The cell pellet was then resuspended with Nuclear Extraction buffer and soluble nuclear proteins were collected by centrifugation at 20,000 *g*. The cytoplasmic fraction was validated by WB for PDGFR-α and the nuclear fraction was validated by WB for HDAC2. For coIP, cell nuclei isolated were resupspended and lysed by IP buffer

containing 1% NP40. After homogenization and centrifugation at 20,000 *g*, the supernatants, containing equal volumes and equal amounts of proteins, were used for coIP. 1-5 μg of anti-p300 (N-15) and 30 μl slurry of Protein G Sepharose 4 Fast Flow (GE17-0618-01; GE Healthcare, Pittsburgh, PA) were used to pulldown p300. After Sepharose beads were washed for 4 times, coprecipitated SMAD2/3 and TAZ were eluted by Laemmli sample buffer (1610737; Bio-Rad, Hercules, CA) for WB.

***Chromatin immunoprecipitation (ChIP)-qPCR:*** Control, p300 knockdown, and C646-incubated HSCs stimulated with TGFβ1 were collected for ChIP using an EZ-Magna-ChIP HiSens kit (17-10461; MilliporeSigma), as we previously described (7). In brief, HSCs were first fixed with 1% formaldehyde to cross-link protein and DNA. Cell lysates were then subjected to sonication for ChIP. ChIP was done using anti-histone H3-acetyl K27 antibody (H3K27AC) (ab4729; Abcam) or control IgG (sc-2027; Santa Cruz Technology). Precipitated DNA fragments containing gene promoter of POSTN or CTGF were detected by qPCR. Primers for POSTN: forward CAAGGAAGCTGATTGTGGTTACC; reverse GCAATCCCTAGCCAAAGGAATG. Primers for CTGF: forward GCTGAGTGTCAAGGGGTCAGG; reverse GGCTCGCCAATGAGCTGAATG.

***HSC/tumor coculture:*** HSCs were seeded into a 24-well cell culture plate and grew to confluence. L3.6 cancer cells, in a single-cell suspension, were added on the top of HSCs so that L3.6 and HSCs grew together. After 3-day-coculture in serum-free DMEM, cells were collected for IF for E-cadherin to label L3.6 cancer cells. IF signals were quantified using an Odyssey imaging System (LI-COR Biosciences, Lincoln, NE).

***HSC/tumor coinjection and in vivo xenogen imaging:*** Experiments were approved by Institutional Animal Care and Use Committee of Mayo Clinic or University of Minnesota. 8-week-old male nude mice (Charles River; 553) were used as tumor implantation recipients. HT29 cells ($0.5 \times 10^6$) were mixed with HSCs ($0.5 \times 10^6$) and they were coinjected into a nude mouse subcutaneously (2, 8). Tumor nodules were measured using a caliper and tumor volumes were calculated: tumor volume = $(\text{width})^2 \times \text{length}/2$. Tumor growth curves were generated with the GraphPad Prism 5 software (GraphPad Software, Inc., La Jolla, CA).

For in vivo xenogen imaging, HT29 expressing firefly luciferase by lentiviral transduction were used for coinjection. Each mouse received 150 µl D-luciferin (GOLDBIO, online shop) by intraperitoneal injection and anesthetized by isoflurane. HT29 bioluminescence was detected and measured by the Xenogen IVIS 200 machine (Caliper Life Sciences, Waltham, MA) and the Living Image software (Caliper Life Sciences) (2, 8).

***Liver metastasis mouse models.*** Experiments were approved by Institutional Animal Care and Use Committee of University of Minnesota. L3.6 liver metastases were generated by portal vein injection. 8 weeks old male SCID mice (Charles River Frederick Research Model Facility) were used as tumor implantation recipients and $1 \times 10^6$ L3.6 cells suspended in 100 µl PBS were used for each injection. Mice were sacrifice 14 days later for isolation of liver metastases. *p300*F/F mice (9) were bred with collagen1A1-*cre* transgenic mice (provided by Dr. Tatiana Kisseleva at UCSD), and pups were genotyped by a PCR-based approach. PCR primer pairs were: 5'- TGG TTA TCG GTT CAC CAT TTT G-3' and 5'- CAG TAG ATG CTA GAG AAA GCC-3'. Littermate-matched *p300*+/+*cre* and *p300*F/F*cre* mice were used for intrasplenic injection of LLCs. $1 \times 10^6$ LLCs suspended in 30 µl PBS were used for each intrasplenic injection. Mice were sacrificed 10 days later for isolation of liver metastases. Detailed portal vein and intrasplenic

injection procedures are included in our prior publications (6, 7).

## References


1. Kang N, Yaqoob U, Geng Z, Bloch K, Liu C, Gomez T, Billadeau D, et al. Focal adhesion assembly in myofibroblasts fosters a microenvironment that promotes tumor growth. Am J Pathol 2010;177:1888-1900.
2. Liu C, Billadeau DD, Abdelhakim H, Leof E, Kaibuchi K, Bernabeu C, Bloom GS, et al. IQGAP1 suppresses TbetaRII-mediated myofibroblastic activation and metastatic growth in liver. J Clin Invest 2013;123:1138-1156.
3. Fujii M, Toyoda T, Nakanishi H, Yatabe Y, Sato A, Matsudaira Y, Ito H, et al. TGF-beta synergizes with defects in the Hippo pathway to stimulate human malignant mesothelioma growth. J Exp Med 2012;209:479-494.
4. Liu C, Li J, Xiang X, Guo L, Tu K, Liu Q, Shah VH, et al. PDGF receptor alpha promotes TGF-beta signaling in hepatic stellate cells via transcriptional and post transcriptional regulation of TGF-beta receptors. Am J Physiol Gastrointest Liver Physiol 2014.
5. Decker NK, Abdelmoneim SS, Yaqoob U, Hendrickson H, Hormes J, Bentley M, Pitot H, et al. Nitric oxide regulates tumor cell cross-talk with stromal cells in the tumor microenvironment of the liver. Am J Pathol 2008;173:1002-1012.
6. Xiang X, Wang Y, Zhang H, Piao J, Muthusamy S, Wang L, Deng Y, et al. Vasodilator-stimulated phosphoprotein promotes liver metastasis of gastrointestinal cancer by activating a β1-integrin-FAK-YAP1/TAZ signaling pathway. npj Precision Oncology 2018;2:2.
7. Dou C, Liu Z, Tu K, Zhang H, Chen C, Yaqoob U, Wang Y, et al. P300 Acetyltransferase Mediates Stiffness-Induced Activation of Hepatic Stellate Cells Into Tumor-Promoting Myofibroblasts. Gastroenterology 2018;154:2209-2221 e2214.
8. Tu K, Li J, Verma VK, Liu C, Billadeau DD, Lamprecht G, Xiang X, et al. VASP promotes TGF-β activation of hepatic stellate cells by regulating Rab11 dependent plasma membrane targeting of TGF-β receptors. Hepatology (Baltimore, Md.) 2015;61:361.
9. Kasper LH, Fukuyama T, Biesen MA, Boussouar F, Tong C, de Pauw A, Murray PJ, et al. Conditional knockout mice reveal distinct functions for the global transcriptional coactivators CBP and p300 in T-cell development. Mol Cell Biol 2006;26:789-809.

**Supplemental Figure Legends**

**Suppl. Fig. 1. P300 knockdown does not influence TGFβ1-induced SMAD phosphorylation and protein levels of TβRII, TβRI and YAP1/TAZ of HSCs. A.** Control and p300 knockdown HSCs were stimulated with TGFβ1 for different times and collected for WB. P300 knockdown did not influence TGFβ1-induced phosphorylation of SMAD2 and protein levels of YAP1 and TAZ. Data are representative of 3 repeats with similar results. **B.** HSCs expressing TβRI-FLAG by retroviral transduction were transduced with control or p300 shRNA lentiviruses. WB revealed that p300 knockdown did not influence protein levels of TβRII and TβRI of HSCs. Data are representative of 3 repeats with similar results.

**Suppl. Fig. 2. Nuclear localization of TAZ-4SA mutant is mediated by p300. A.** NIH3T3 cells expressing doxycycline-inducible FLAG-TAZ-4SA were treated with DMSO or C646 for 24 hours and collected for IF for FLAG (left) and nuclear fractionation (right). C646 inhibited nuclear targeting of FLAG-TAZ-4SA. *, $P<0.05$ by *t*-test, n=3 repeats. Bar, 50 μm. **B.** NIH3T3 cells expressing doxycycline-inducible FLAG-TAZ-4SA were transduced with NT shRNA or p300 shRNA lentiviruses and collected for IF for FLAG (left) and nuclear fractionation (right). P300 shRNA inhibited nuclear targeting of FLAG-TAZ-4SA mutant. *, $P<0.05$ by *t*-test, n=3 repeats. Bar, 50 μm.

**Suppl. Fig. 3. Nuclear localization of YAP1-5SA mutant is minimally affected by p300. A.** NIH3T3 cells expressing doxycycline-inducible FLAG-YAP1-5SA were treated with DMSO or C646 for 24 hours and collected for IF for FLAG and nuclear fractionation. C646 minimally affected nuclear targeting of FLAG-YAP1-5SA mutant. $P>0.05$ by *t*-test, n=3 repeats. Bar, 50 μm. **B.** NIH3T3 cells expressing doxycycline-inducible FLAG-YAP1-5SA were transduced with NT shRNA or p300 shRNA lentiviruses and collected for IF for FLAG and nuclear fractionation.

P300 shRNA minimally affected nuclear targeting of FLAG-YAP1-5SA. $P>0.05$ by *t*-test, n=3 repeats. Bar, 50 μm.

**Suppl. Fig. 4. TGFβ1 induction of tumor-promoting factors was inhibited by knockdown of both TAZ and YAP1. A.** HSCs transfected by control or TAZ siRNA were treated with TGFβ1 and collected for WB. TGFβ1-induced upregulated of α-SMA and fibronectin was not significantly influenced by TAZ knockdown alone. $P>0.05$ by ANOVA, n=3 repeats. **B.** HSCs transfected by both TAZ and YAP1 siRNA and collected for WB. TGFβ1 induction of α-SMA and 4 tumor-promoting factors was significantly reduced by TAZ/YAP1 siRNA. *, $P<0.05$ by ANOVA, n=3 repeats.

**Suppl. Fig. 5. P300 facilitates gene expression by acetylating histones. A.** Microarray analysis using Human HT-12 v4 Expression BeadChip identified more than 700 TGFβ1-inducible genes. Representative 22 TGFβ1-inducible genes are shown. **B.** HSC conditioned medium (CM) was used as a stimulant for HT29 cells in MTS proliferation assay. CM of p300 knockdown HSCs was less effective than that of control cells at promoting HT29 proliferation, and the impaired tumor-promoting effect of p300 knockdown HSCs was partially rescued by CTGF. *, $P<0.05$ by ANOVA, n=5. **C.** HSCs stimulated with TGFβ1 were collected for ChIP-qPCR to study acetylation of histone 3 on POSTN and CTGF promoter. C646 suppressed H3K27Ac on the promoter of POSTN and CTGF gene in TGFβ1-stimulated HSCs. *, $P<0.05$ by ANOVA, n=3.

**Suppl. Fig. 6. C646 suppresses tumor growth by inhibiting myofibroblasts. A.** Cell proliferation assay showed that C646 at 20 μM did not influence HT29 cell proliferation *in vitro*. **B.** and **C.** Tumor nodules were used for double IF for α-SMA and SMAD2/3. Nuclear SMAD2/3 of tumor myofibroblasts were reduced by C646. *, $P<0.05$ by *t*-test, n>60 cells per

group. Bar, 20 μm. **S**: stroma; **T**: tumor. **D.** Nuclear TAZ in tumor myofibroblasts was also reduced by C646. *, $P<0.05$ by *t*-test, n>60 cells per group. Bar, 20 μm. **S**: stroma; **T**: tumor.

**Suppl. Fig. 7. C646 suppresses tumor growth by inhibiting myofibroblasts. A.** IF revealed that TGFβ transcriptional targets of HSCs, periostin and tenascin C, were reduced by C646 treatment in tumors. *, $P<0.05$ by *t*-test, n=3 tumors per group. Bar, 100 μm. **B.** α-SMA IF revealed reduced myofibroblast densities in tumors arising from HT29/HSC-p300shRNA coinjections compared to control coinjections. *, $P<0.05$ by *t*-test, n=4 tumors per group. Bar, 100 μm.

**Suppl. Fig. 8. Nuclear TAZ in myofibroblasts of liver metastases is downregulated by *cre*-mediated p300 gene disruption. A.** Metastases were assessed by IF using antibodies against TAZ in conjunction with either desmin to mark quiescent HSCs or α-SMA to mark activated-HSC/myofibroblasts. TAZ was increased in activated-HSC/myofibroblasts (arrows) of liver metastases than in HSCs (arrowheads). *, $P<0.05$ by *t*-test, n>36 cells. Bar, 20 μm. **S**: stroma; **T**: tumor. **B.** α-SMA IF was used to label myofibroblasts of liver metastases. TAZ was reduced in *p300*F/F*cre* myofibroblasts (arrows) than in *p300*+/+*cre* myofibroblasts (arrowheads). *, $P<0.05$ by *t*-test, n>45 cells. Bar, 20 μm. **S**: stroma; **T**: tumor.

**Suppl. Fig. 9. TGFβ-inducible and stiffness-inducible targets are distinct but with a small overlap. A.** Out of 23 tumor-promoting targets of stiffness that we identified by RNA-seq previously, only IL11. THBS1, SERPINE1, FGF2, and CTGF are TGFβ1-inducible genes, as revealed by RNA-seq (GSE127964). **B.** Out of 5 tumor-promoting targets of TGFβ1 identified in this study, only CTGF and FGF2 are upregulated by stiffness, as revealed by RNA-seq (GSE101343). *, $P<0.05$ by Bonferroni post hoc test.

Suppl. Fig. 1

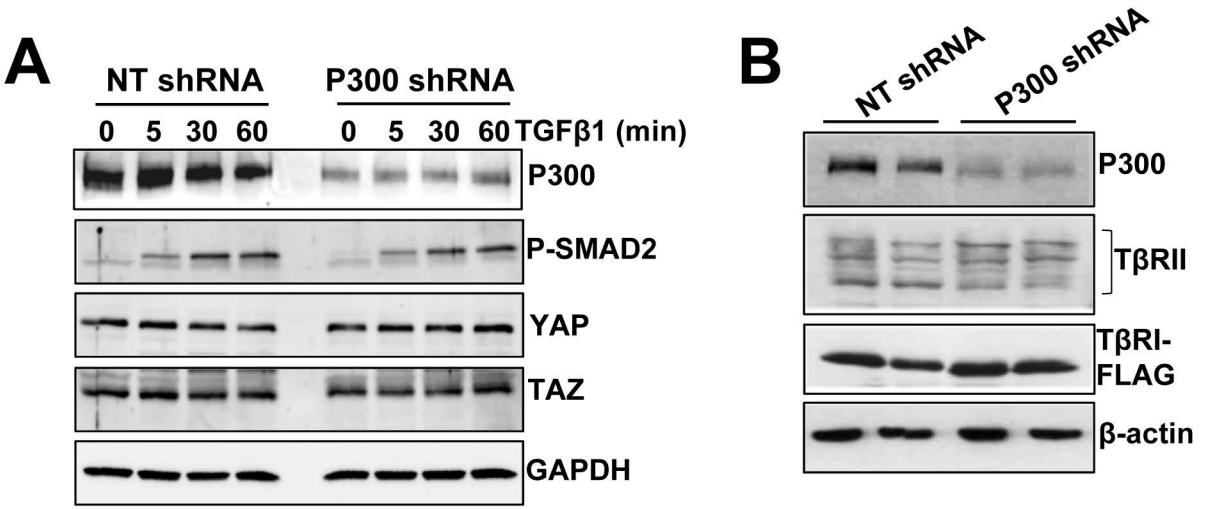
A
NT shRNA
P300 shRNA
0 5 30 60 0 5 30 60 TGFβ1 (min)
P300
P-SMAD2
YAP
TAZ
GAPDH
B
NT shRNA
P300 shRNA
P300
TβRII
TβRI-FLAG
β-actin

Suppl. Fig. 2

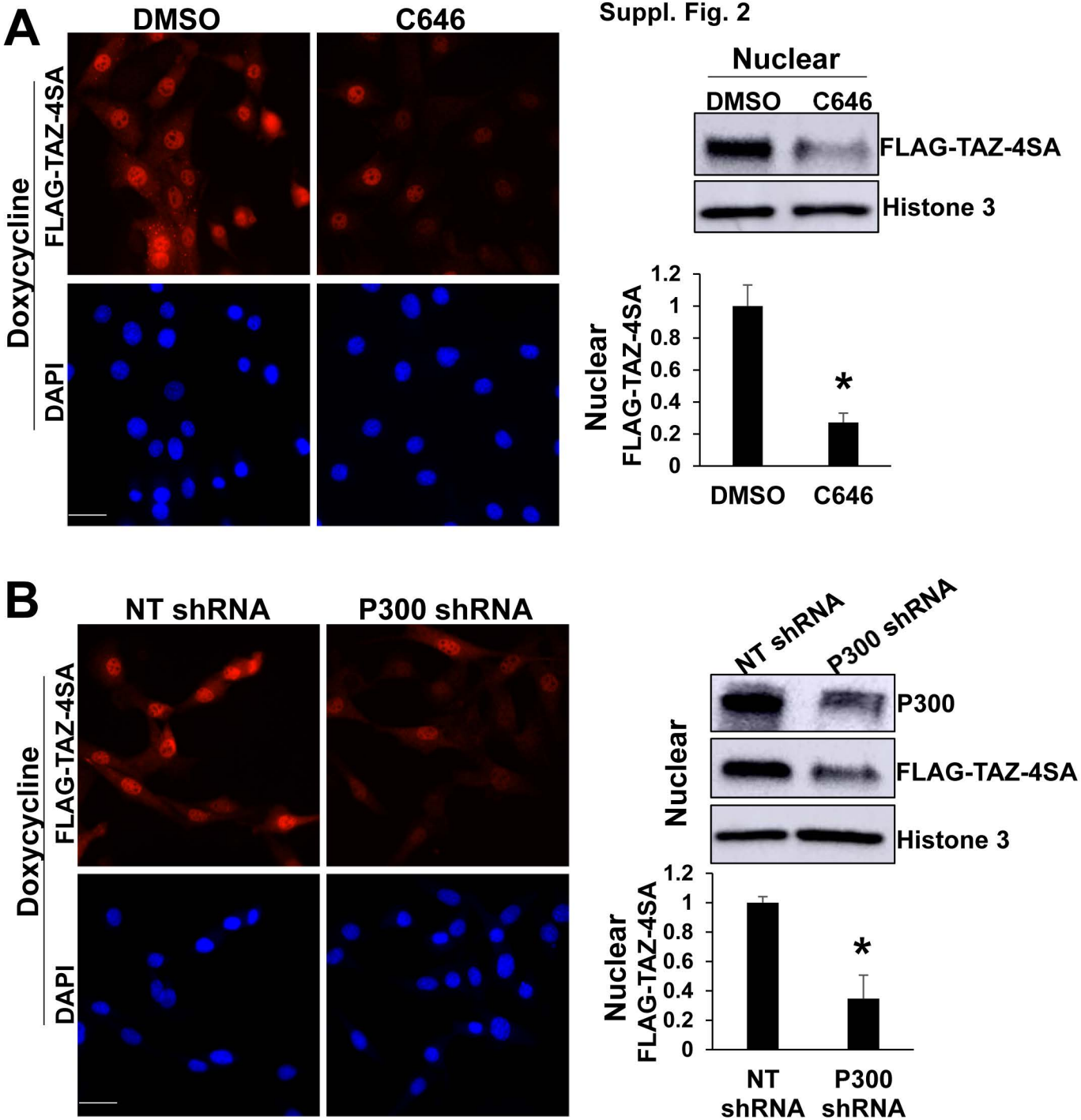
A
DMSO
C646
Doxycycline
FLAG-TAZ-4SA
DAPI
Nuclear
DMSO
C646
FLAG-TAZ-4SA
Histone 3
Nuclear FLAG-TAZ-4SA
1.2
1
0.8
0.6
0.4
0.2
0
*
DMSO
C646
B
NT shRNA
P300 shRNA
Doxycycline
FLAG-TAZ-4SA
DAPI
NT shRNA
P300 shRNA
Nuclear
P300
FLAG-TAZ-4SA
Histone 3
Nuclear FLAG-TAZ-4SA
1.2
1
0.8
0.6
0.4
0.2
0
*
NT shRNA
P300 shRNA

Suppl. Fig. 3

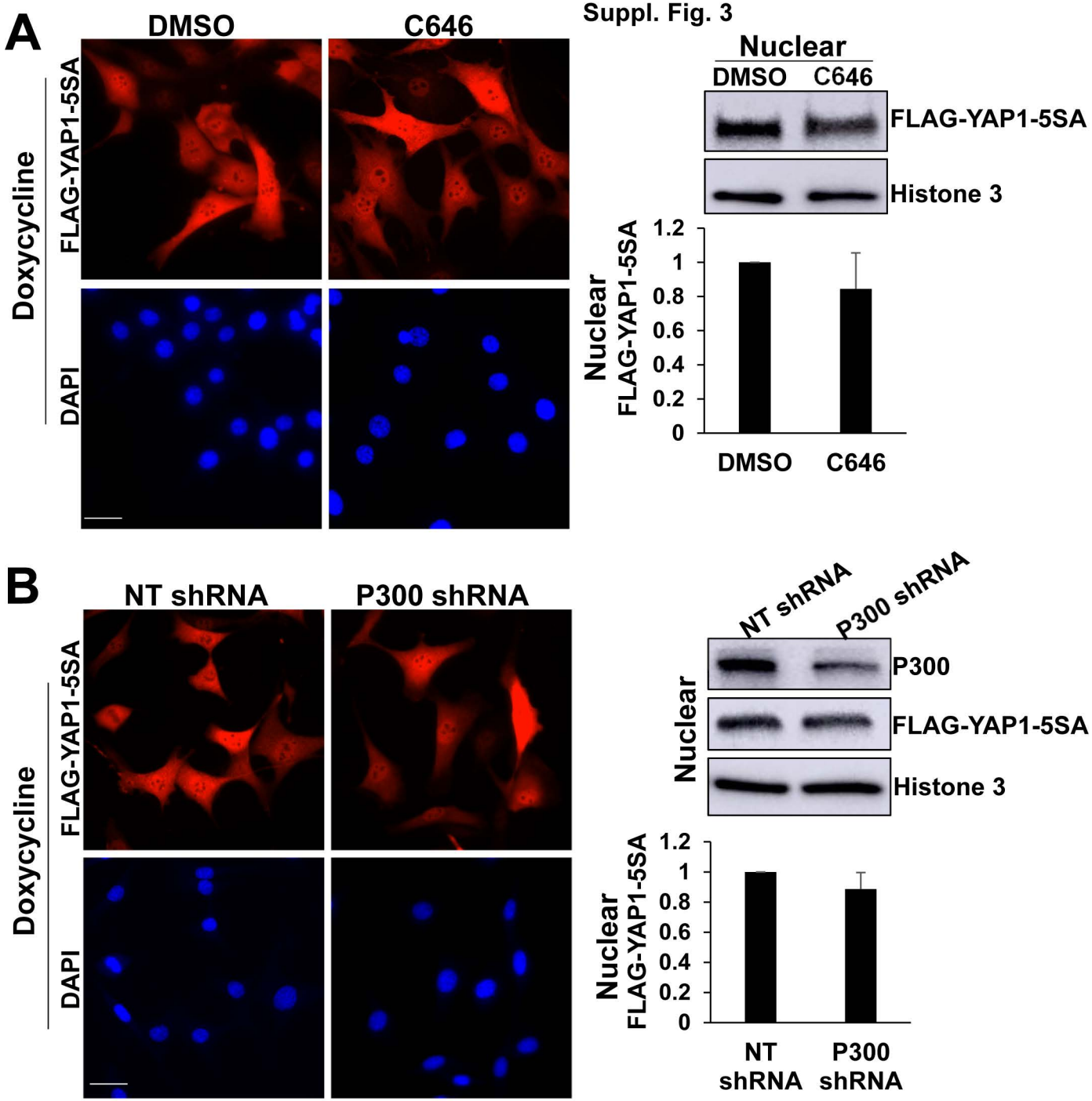
A
DMSO
C646
Doxycycline
FLAG-YAP1-5SA
DAPI
Nuclear
DMSO
C646
FLAG-YAP1-5SA
Histone 3
Nuclear FLAG-YAP1-5SA
1.2
1
0.8
0.6
0.4
0.2
0
DMSO
C646
B
NT shRNA
P300 shRNA
Doxycycline
FLAG-YAP1-5SA
DAPI
NT shRNA
P300 shRNA
Nuclear
P300
FLAG-YAP1-5SA
Histone 3
Nuclear FLAG-YAP1-5SA
1.2
1
0.8
0.6
0.4
0.2
0
NT shRNA
P300 shRNA

Suppl. Fig. 4

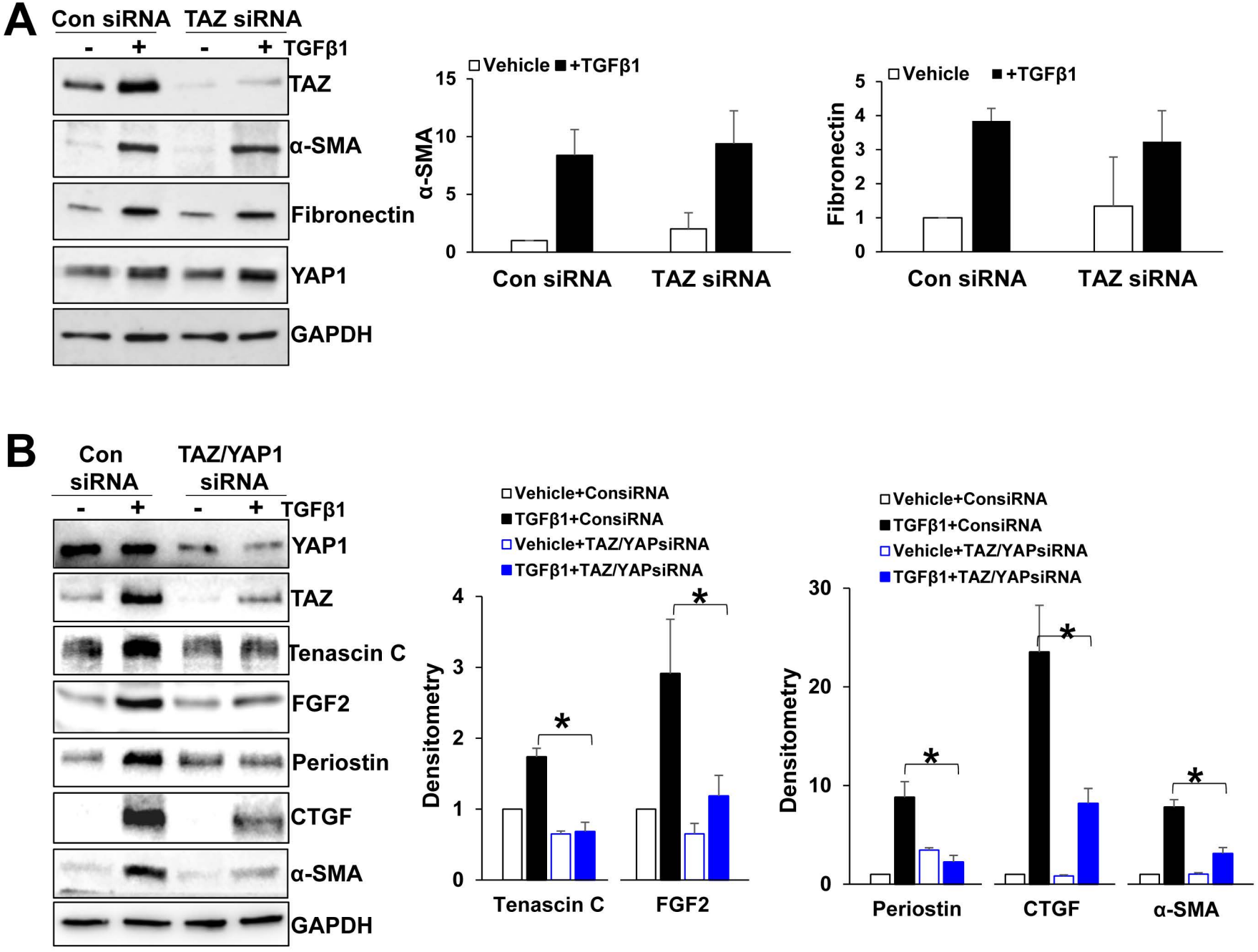
A
Con siRNA
TAZ siRNA
- + - + TGFβ1
TAZ
α-SMA
Fibronectin
YAP1
GAPDH
Vehicle +TGFβ1
α-SMA
Con siRNA
TAZ siRNA
Vehicle +TGFβ1
Fibronectin
Con siRNA
TAZ siRNA
B
Con siRNA
TAZ/YAP1 siRNA
- + - + TGFβ1
YAP1
TAZ
Tenascin C
FGF2
Periostin
CTGF
α-SMA
GAPDH
Vehicle+ConsiRNA
TGFβ1+ConsiRNA
Vehicle+TAZ/YAPsiRNA
TGFβ1+TAZ/YAPsiRNA
Densitometry
Tenascin C
FGF2
Vehicle+ConsiRNA
TGFβ1+ConsiRNA
Vehicle+TAZ/YAPsiRNA
TGFβ1+TAZ/YAPsiRNA
Densitometry
Periostin
CTGF
α-SMA

Suppl. Fig. 5

**A**

| Gene | mRNA fold increase by TGFβ1 |
|---|---|
| IGFBP3 | 11 |
| TAGLN(SM22-α) | 4.33 |
| SERPINE1(PAI-1) | 5.99 |
| GADD45B | 6.5 |
| **ACTA2(α-SMA)** | **6.3** |
| CNN1(Calponin1) | 5.3 |
| **CTGF** | **2.3** |
| ITGA1 | 4.6 |
| **TNC** | **3** |
| MMP3 | 3 |
| Col7A | 2.76 |
| KLF10 | 1.87 |
| SMAD7 | 1.82 |
| **PDGFC** | **2.37** |
| Col8A2 | 2.0 |
| MYL9 | 2.6 |
| FAP | 2.4 |
| ECGF | 2.33 |
| MMP10 | 2.06 |
| FN1 | 2.01 |
| **FGF2** | **1.98** |
| **POSTN** | **1.6** |

**GSE116509**

**B**

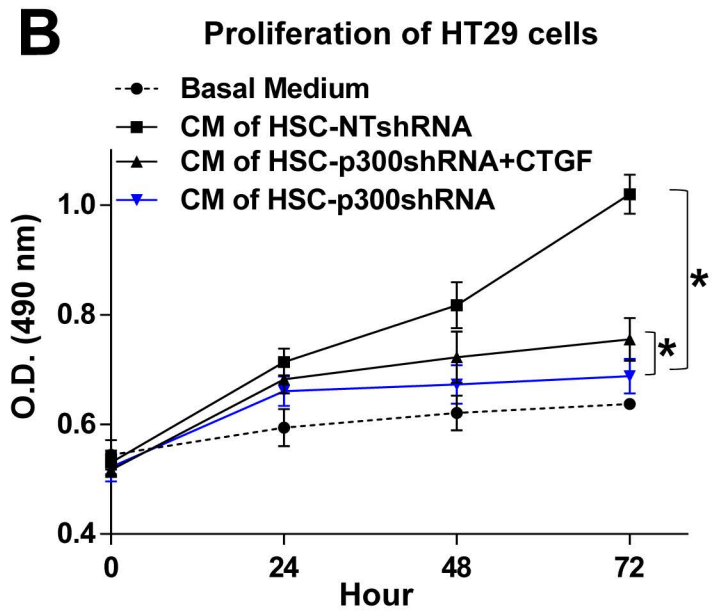


**C**

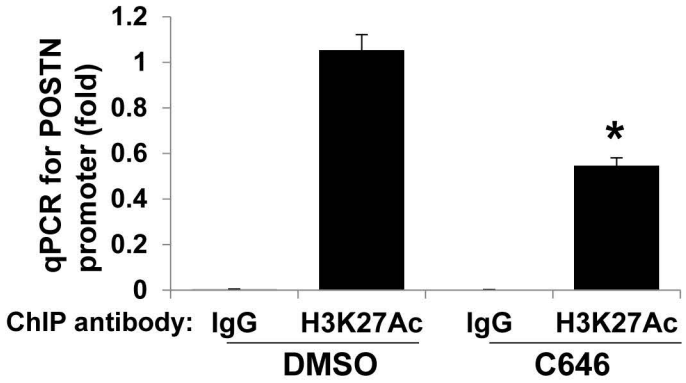


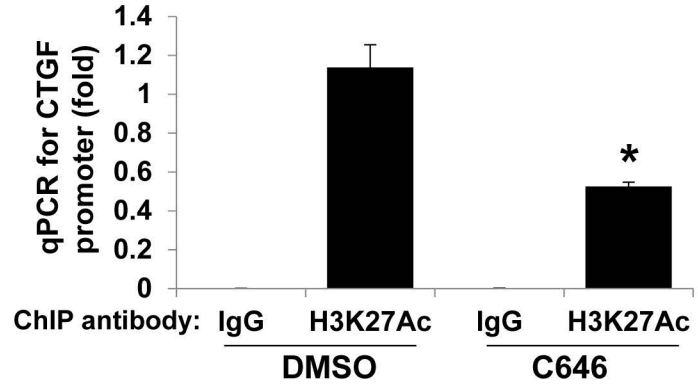

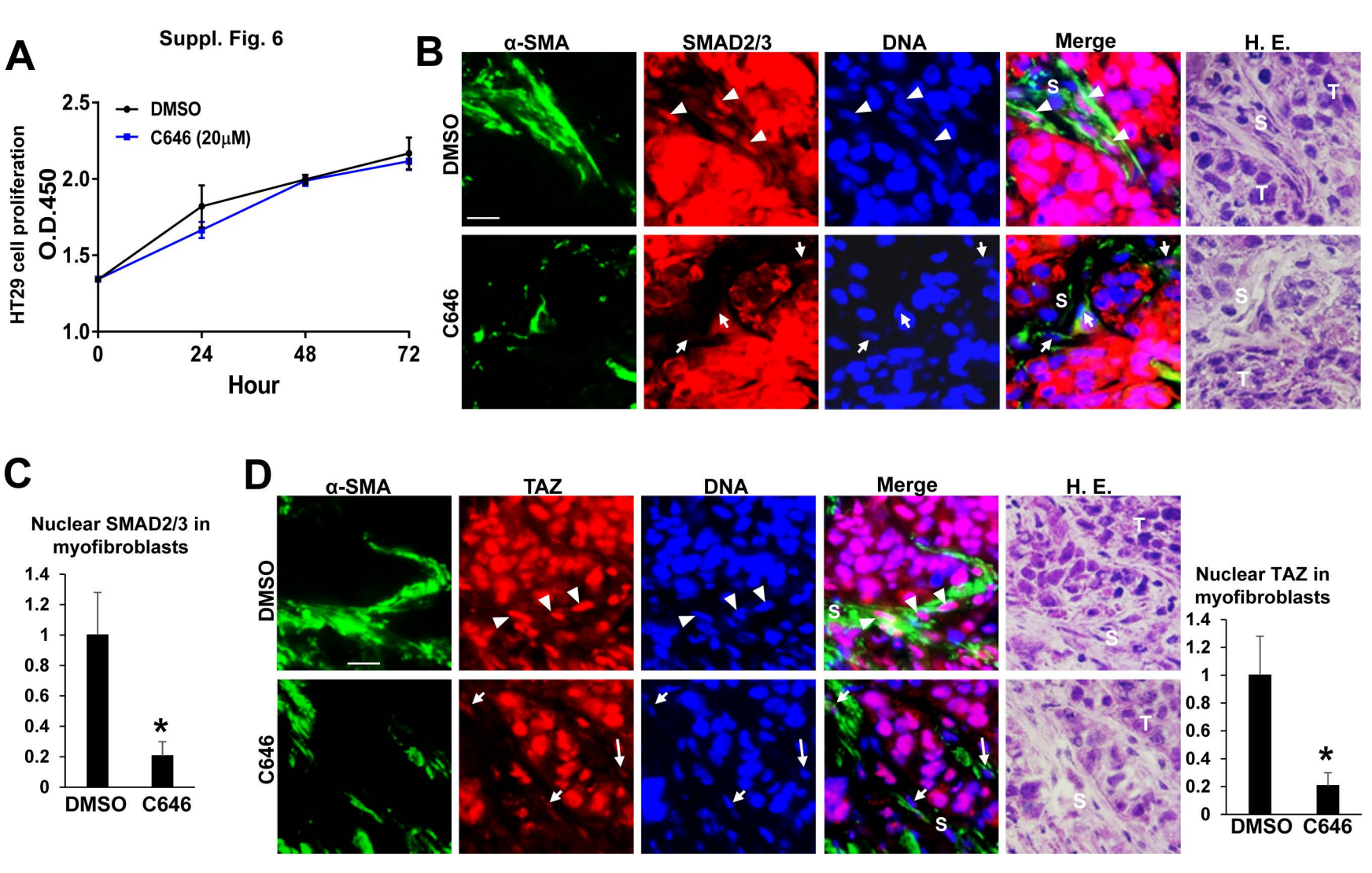
Suppl. Fig. 6
A
HT29 cell proliferation
O.D.450
2.5
2.0
1.5
1.0
DMSO
C646 (20μM)
0
24
48
72
Hour
B
α-SMA
SMAD2/3
DNA
Merge
H. E.
DMSO
C646
S
T
C
Nuclear SMAD2/3 in myofibroblasts
1.4
1.2
1
0.8
0.6
0.4
0.2
0
*
DMSO
C646
D
α-SMA
TAZ
DNA
Merge
H. E.
DMSO
C646
Nuclear TAZ in myofibroblasts

Suppl. Fig. 7

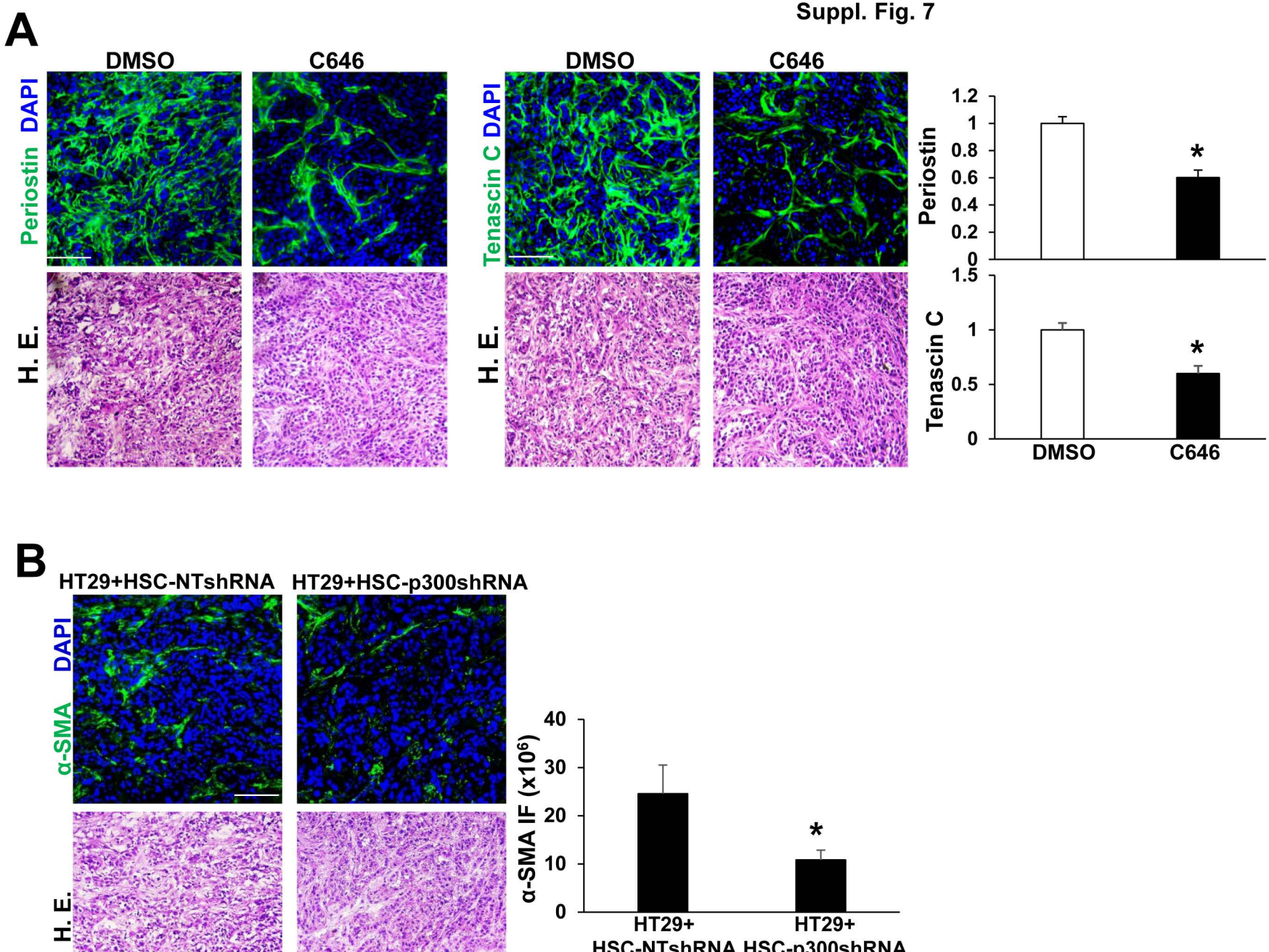
A
DMSO
C646
Periostin DAPI
H. E.
Tenascin C DAPI
Periostin
Tenascin C
1.2
1
0.8
0.6
0.4
0.2
0
1.5
0.5
*
DMSO
C646
B
HT29+HSC-NTshRNA
HT29+HSC-p300shRNA
α-SMA DAPI
H. E.
α-SMA IF (x10^6)
40
30
20
10
0
HT29+ HSC-NTshRNA
HT29+ HSC-p300shRNA

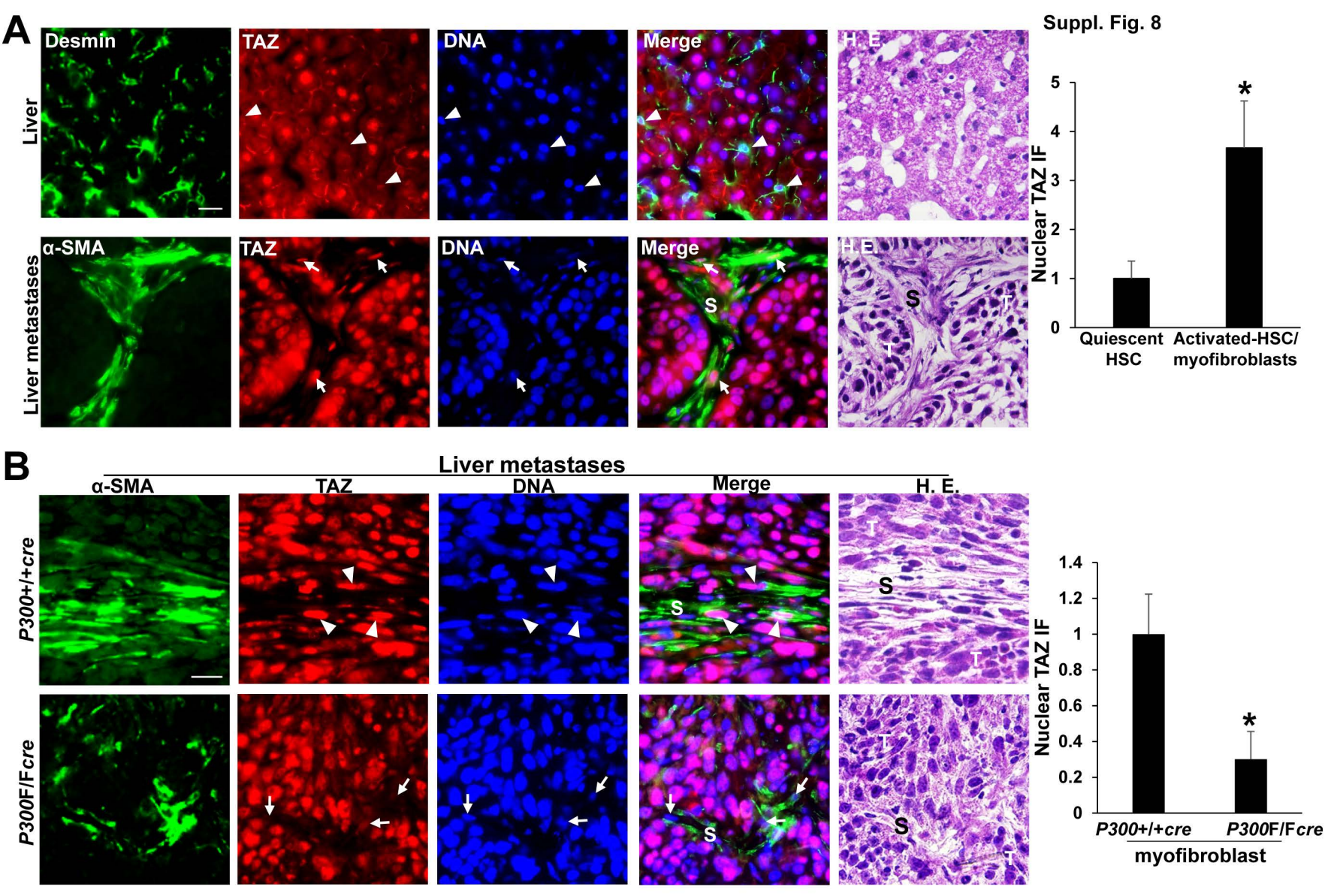
Suppl. Fig. 8
A
Desmin
TAZ
DNA
Merge
H. E.
Liver
α-SMA
TAZ
DNA
Merge
H. E.
Liver metastases
S
T
Nuclear TAZ IF
5
4
3
2
1
0
*
Quiescent HSC
Activated-HSC/ myofibroblasts
B
Liver metastases
α-SMA
TAZ
DNA
Merge
H. E.
P300+/+cre
P300F/Fcre
S
T
Nuclear TAZ IF
1.4
1.2
1
0.8
0.6
0.4
0.2
0
*
P300+/+cre
P300F/Fcre
myofibroblast

Suppl. Fig. 9

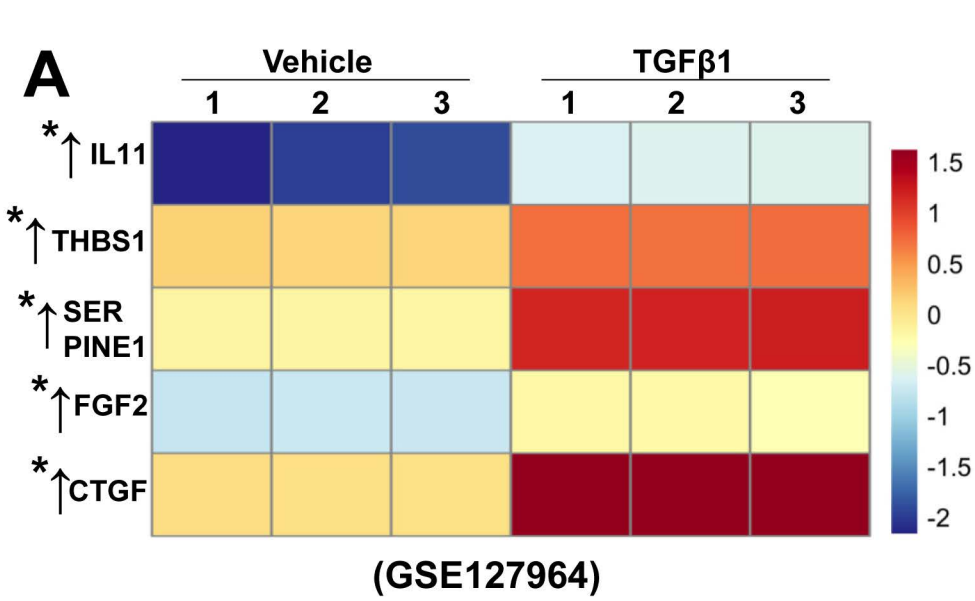


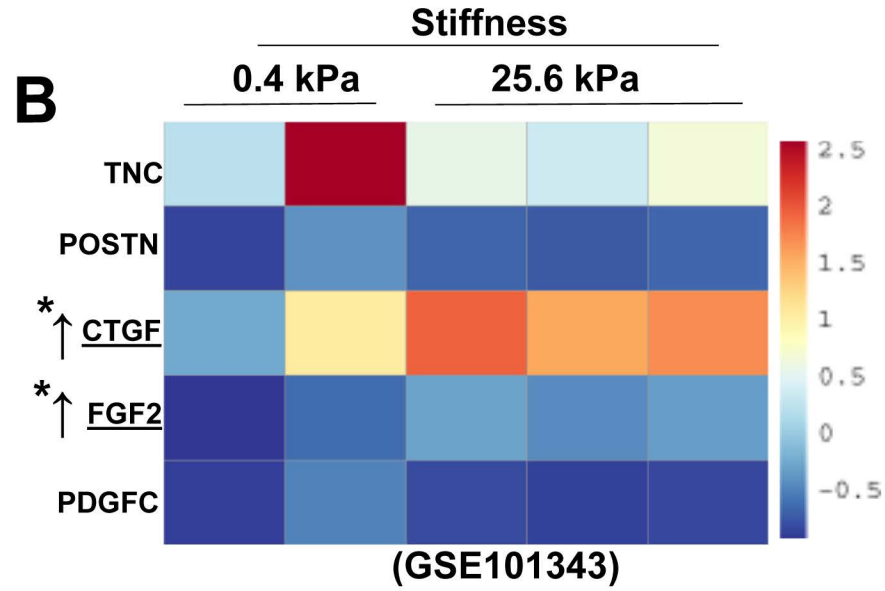


*, $P<0.05$ by Bonferroni post hoc test